Molecular BioSystems

View Online
Dynamic Article Links

Cite this: *Mol. BioSyst.*, 2011, **7**, 2577–2588

www.rsc.org/molecularbiosystems

PAPER

A metabolic system-wide characterisation of the pig: a model for human physiology

Claire A. Merrifield,[a] Marie Lewis,[b] Sandrine P. Claus,[ad] Olaf P. Beckonert,[a] Marc-Emmanuel Dumas,[a] Swantje Duncker,[c] Sunil Kochhar,[c] Serge Rezzi,[c] John C. Lindon,[a] Mick Bailey,[b] Elaine Holmes*[a] and Jeremy K. Nicholson[a]

Received 22nd January 2011, Accepted 12th May 2011
DOI: 10.1039/c1mb05023k

The pig is a single-stomached omnivorous mammal and is an important model of human disease and nutrition. As such, it is necessary to establish a metabolic framework from which pathology-based variation can be compared. Here, a combination of one and two-dimensional ^{1}H and ^{13}C nuclear magnetic resonance spectroscopy (NMR) and high-resolution magic angle spinning (HR-MAS) NMR was used to provide a systems overview of porcine metabolism *via* characterisation of the urine, serum, liver and kidney metabolomes. The metabolites observed in each of these biological compartments were found to be qualitatively comparable to the metabolic signature of the same biological matrices in humans and rodents. The data were modelled using a combination of principal components analysis and Venn diagram mapping. Urine represented the most metabolically distinct biological compartment studied, with a relatively greater number of NMR detectable metabolites present, many of which are implicated in gut-microbial co-metabolic processes. The major inter-species differences observed were in the phase II conjugation of extra-genomic metabolites; the pig was observed to conjugate *p*-cresol, a gut microbial metabolite of tyrosine, with glucuronide rather than sulfate as seen in man. These observations are important to note when considering the translatability of experimental data derived from porcine models.

Introduction

The relevance of using the pig (*Sus scrofa*) as an experimental animal model can be seen on a number of levels. Experimentally, the pig has been described as the 'best non-primate model for studying human nutrition'[1] and tolerance to food antigens (Ag),[2] as it is a large single-stomached omnivore and has a comparable gut physiology to humans. It has also been used extensively as a model for a variety of human disease risk factors including obesity, stress and diabetes and for studies of drug metabolism.[3] Sequencing of the pig genome is underway and comparative maps show extensively conserved homology with the human genome.[4,5] Its economical and agricultural importance as a food source, coupled with biomedical interest in using the pig as a source for xenotransplantation and surgical development, has resulted in an extensive knowledge base regarding porcine genomics, reproduction, immunology and development.[6] The development of transgenic pigs[7] reinforces their suitability as a model for research into human physiology and disease processes. Therefore, because of its relevance to human disease and nutrition, and the fact that multi-level information (transcriptomic, metagenomic, immunological) is available allowing a holistic systems overview to be attained, it is of general interest to characterise porcine metabolism as fully as possible and its normal physiological variation, and to compare this information with what is known for humans.

Here we have used a metabolic profiling strategy to define the metabolic phenotype of the pig. Metabonomics, based on high resolution spectroscopic profiling and mathematical modelling has been used to phenotype a wide range of species, including mouse, rat, dog, invertebrate, primate and humans, exposed to different physiological and pathological stimuli.[8] Metabolic phenotypes of biofluids and tissues can be generated from nuclear magnetic resonance (NMR) spectroscopic or mass spectroscopic (MS) information, and from these, the influence of genetic diversity, diet and environment can be derived, including contributions from xenobiotics and their metabolites. Thus it is important to establish a metabolic baseline against which pathology-related variation across the organism can be compared.

Metabolic profiles of the two most widely used biofluids (urine and serum), together with the two main organs responsible for

[a] *Biomolecular Medicine, Department of Surgery and Cancer, Imperial College London, UK SW7 2AZ. E-mail: elaine.holmes@imperial.ac.uk*
[b] *Infection and Immunity, Department of Clinical Veterinary Science, University of Bristol, Langford House, Langford, North Somerset, UK BS40 5DU*
[c] *Nestlé Research Centre, Vers-chez-les-Blanc, 1000 Lausanne 26, Switzerland*
[d] *Department of Food and Nutritional Sciences, University of Reading, Whiteknights, Reading, UK RG6 6AP*

metabolism of endogenous and xenobiotic compounds (liver and kidney), of the pig have been examined using 800 MHz ^{1}H nuclear magnetic resonance (NMR) spectroscopy and 800 MHz high-resolution magic angle spinning (HR-MAS) ^{1}H NMR spectroscopy. The pigs used for this baseline study had a controlled diet from weaning, including a diet switch, which is common practice for commercially reared pigs. They also received a small amount of adjuvant two weeks prior to tissue collection, which is comparable to a vaccination. Metabolite assignments have been made using a variety of two-dimensional homo- and heteronuclear NMR techniques, statistical spectroscopic correlation tools and reference to databases of spectra of authentic compounds.

Results

800 MHz 1D ^{1}H NMR partially annotated spectra (Fig. 1) provide an overview of the metabolic profiles from the four matrices (urine, serum, liver, kidney). These are supplemented by further information acquired from a series of 2D spectroscopic experiments in order to reduce peak overlap which inevitably occurs in highly complex biological fluids and tissues, typical examples are shown in Fig. 2 and 3.

Putative assignments were made based on expected coupling constants and carbon shifts only if all of the associated NMR resonances were visible. A table is shown highlighting the major NMR-visible metabolites in each compartment, which were present in sufficient abundance to be detectable by 2D NMR (Table 1).

Cross-compartmental comparisons

A comparison of the NMR-visible metabolites in the different matrices was performed to identify metabolites that are ubiquitously present (*i.e.* core metabolites) and those that are specific to a particular biological compartment. A Venn diagram (Fig. 4) was used to gain a better picture of the porcine system as defined by the four chosen biomatrices and to visualise the metabolic overlap between serum, liver, kidney and urine. A total of 22 core metabolites were found to be present across all 4 biological matrices including several amino acids, choline, glucose and acetate; acetate is a metabolite central to many host metabolic processes but is also produced by many species of bacteria. These core metabolites are mainly related to energy metabolism and protein degradation and, as such, would be expected to be present in all matrices studied. Each tissue also had a unique set of metabolites in addition to the core metabolome.

Urine

Urine was found to be the most different of the biological matrices studied, with 20 urine-specific metabolites including metabolites involved in amino acid, carbohydrate and nucleoside metabolism, and at least 9 metabolites implicated in gut-microbial co-metabolism.[26–32]

This dissimilarity of the urinary metabolic phenotype compared with phenotypes of the other biological compartments can be further visualised using multivariate data analysis. The ^{1}H NMR metabolic profiles of urine, serum, liver and kidney from all seven animals (acquired on a 600 MHz spectrometer) were modelled together using principal components analysis (PCA) to visualise the major sources of variation in the data (Fig. 5). The urine samples separate from the other matrices on the 1st principal component (PC) (Fig. 5A) which accounts for 28% of the total variance of the model, and the difference between urine and the other biological matrices is ascribed primarily to increased levels of aromatic metabolites which have been associated with gut-microbial co-metabolism such as hippurate,[9] indoleacetylglycine, phenylacetylglycine and *p*-cresol glucuronide as well as the methylamines[10–15] (Fig. 5B).

The differences between the other three compartments are explained by PC2 (18% of variance) (Fig. 5C) and 3 (14% of variance) (Fig. 5D) and are mainly due to differing levels of endogenous mammalian metabolites such as glucose, choline, glycerophosphocholine and glutamate. It is also noted that the metabolic variance between individual animals was much less than the variation between the different sample matrices, as evidenced by the clusters visible in Fig. 5A.

Serum

The serum metabolic profile of the pig showed remarkable compositional similarity to that of human plasma as reported by Nicholson *et al.* in 1995[16] and is dominated by resonances from lipid moieties, amino acids, choline metabolites and glucose. NMR-detectable resonances visible in serum but not in the other matrices studied include albumin lysyl, cholesterol and pyruvate.

Liver

The liver metabolite profile was dominated by choline and its phosphorylated derivatives along with glucose, glycogen, triglycerides and amino acids, and displayed visual and compositional similarity to human liver biopsies[17] and rat liver.[18] Unique metabolites observed in the liver included glycogen, observed in humans and rats, and ascorbate and glutathione, well-known antioxidants.[19]

Kidney

The kidney contains NMR detectable quantities of serine, cysteine and glycolate unlike the other matrices studied. In this tissue, effects due to deuteration of the sample were observed in the rotor over the course of the experiment mainly with respect to the alanine resonance as observed previously.[20]

Discussion

The pig is an important model for human disease and this work serves as a template for further disease based metabonomic studies in this valuable test species. The metabolic phenotype for the two most widely used biofluids: urine and serum, and the two main metabolic organs: the liver and kidney, has been comprehensively elucidated using one and two-dimensional 800 MHz NMR and 800 MHz HR-MAS-NMR spectroscopy. Analysis of the relative distribution of metabolites has uncovered a 'core metabolome' stretching across the different biological matrices, comprising mainly amino acids and sugars, indicating that the predominant metabolites present in all four matrices represent energy metabolism and protein degradation.

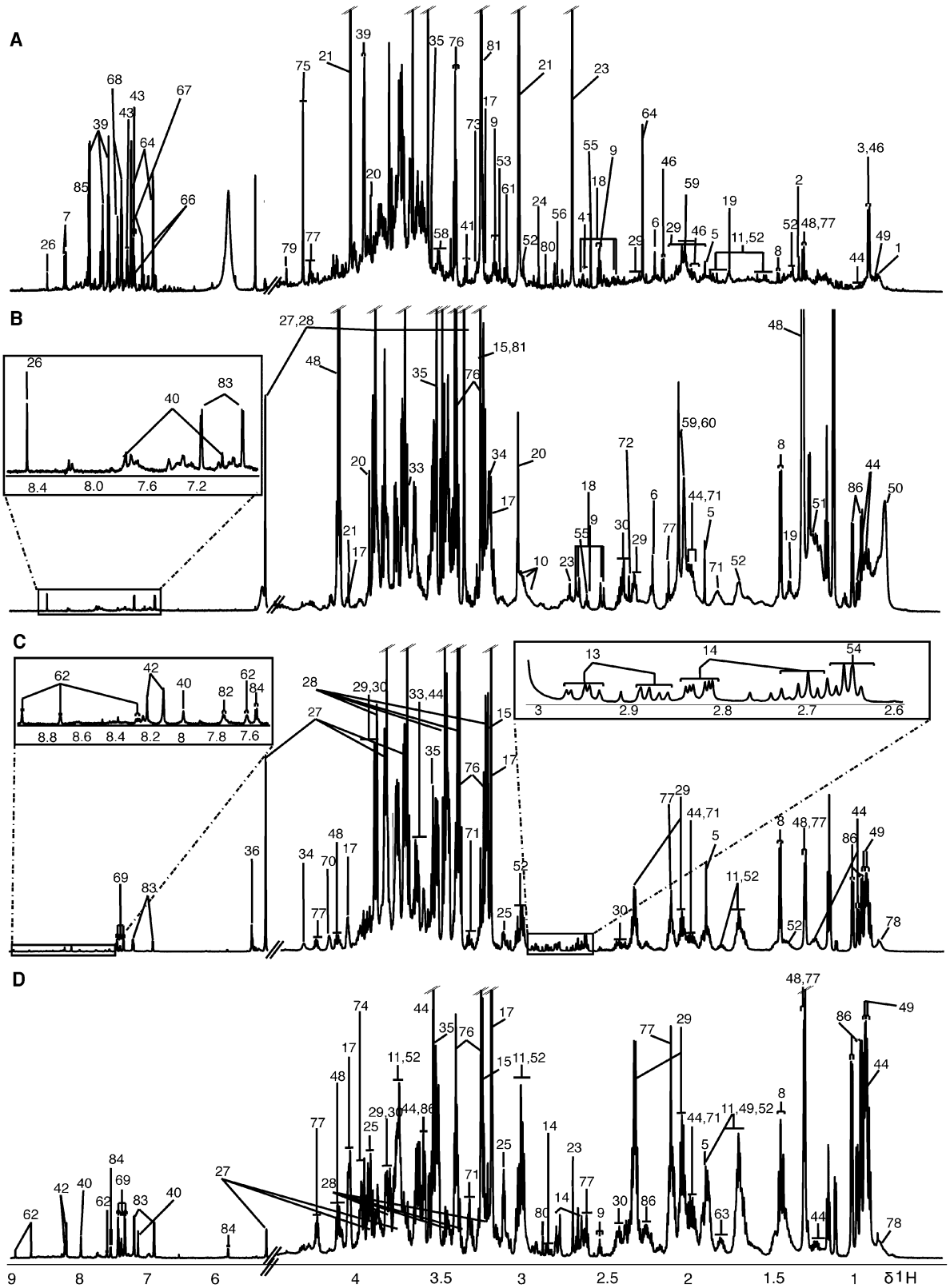

Fig. 1 (A) 800 MHz 1D ^{1}H NMR spectrum of urine partially labelled according to the assignments given in Table 1, (B) 800 MHz CPMG ^{1}H NMR spectrum of serum, (C) 800 MHz CPMG ^{1}H NMR spectrum of liver, (D) 800 MHz CPMG ^{1}H NMR spectrum of kidney. Key as indicated by Table 1.

The composition of the NMR metabolic profiles of the pig were similar to that characterised in the literature for humans and rodents.[16–18] It is complex to quantitatively compare results from tissues from each species, as there are potential

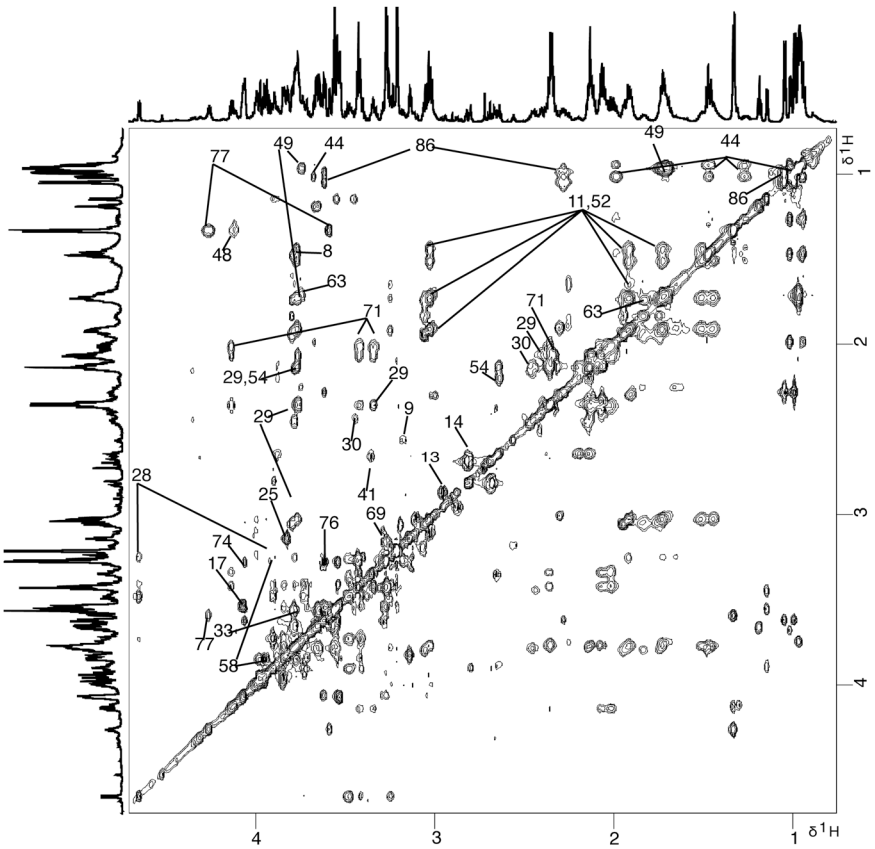

Fig. 2 800 MHz HR-MAS ^{1}H–^{1}H TOCSY NMR spectrum of kidney cortex. Key as indicated by Table 1.

concentration inaccuracies resulting from tissue degradation due to enzymatic activity in the MAS rotor.[21] Tissue extraction techniques could provide a more accurate measure of concentration, but require standardisation between laboratories since different extraction techniques result in a different yield of metabolite concentrations, and access to human tissue samples is limited due to ethical reasons.

Urine shows the most different profile of all of the matrices studied, possibly due to the reduced need for homeostatic control and it is therefore potentially the best metabolic diagnostic matrix in the pig, as observed in other species.[22] So far, no species-specific metabolite profile signatures have been identified that can be readily detected by NMR in these biological matrices, except from in the urinary excretion profile. In urine, the only differences qualitatively observed are in the abundance, relative to humans and rodents, and phase II conjugation of the compounds produced by microbial fermentation of dietary substrates observed in the urine such as *p*-cresol glucuronide, indoleacetylglycine and phenylacetylglycine.[10,23]

Excretion of methylamines in the urine is generally considered to represent gut-microbial degradation of dietary choline, and thus these metabolites are influenced by both diet and gut microbial metabolic activity.[14,24] Phenylacetate, *p*-cresol and indoleacetate are the major microbial fermentation products of dissimilatory amino acid metabolism in the gut. Their production and subsequent conjugation and excretion in the urine requires the presence of diet-derived precursors; phenylalanine, tyrosine and tryptophan respectively.[15] Hippurate is glycine conjugated benzoic acid and therefore its presence in the urine is either directly related to ingestion of benzoic acid or gut microbial fermentation of dietary phenols to form benzoic acid followed by conjugation.[9] Many of the 'unique' metabolites present in urine can therefore be directly attributed to both the diet and the actions of microbial metabolism on the diet and their presence and abundance is expected to change dependant on experimental design.

In this protocol, the pigs underwent a diet switch, common to commercially reared animals and also received antigen with an adjuvant, which we consider to be equivalent to a vaccination such as young pigs and humans routinely receive. Given the time period that elapsed between adjuvant administration and tissue and biofluid sampling, it is highly unlikely that the adjuvant had any metabolic consequences. However, we can speculate that the composition of the urinary metabolic profile is likely to change based on the diet and gut microbial composition of the animal. The animals in this study were young, and had yet to undergo sexual maturation, and a dedicated study would be necessary to confirm the metabolic changes associated with ageing in the pig. A number of studies have looked at metabolic changes over time in the rodent and human, but the results are species-specific and may be gender-dependent.[22,25]

Inter-species differences in phase II conjugation of microbial co-metabolites

The major metabolite of dietary tryptophan in the pig is indoleacetylglycine and was present only in urine; this is in contrast with rodents and humans, who generally excrete indoxylsulfate[26,27] from bacterial indole production.[28]

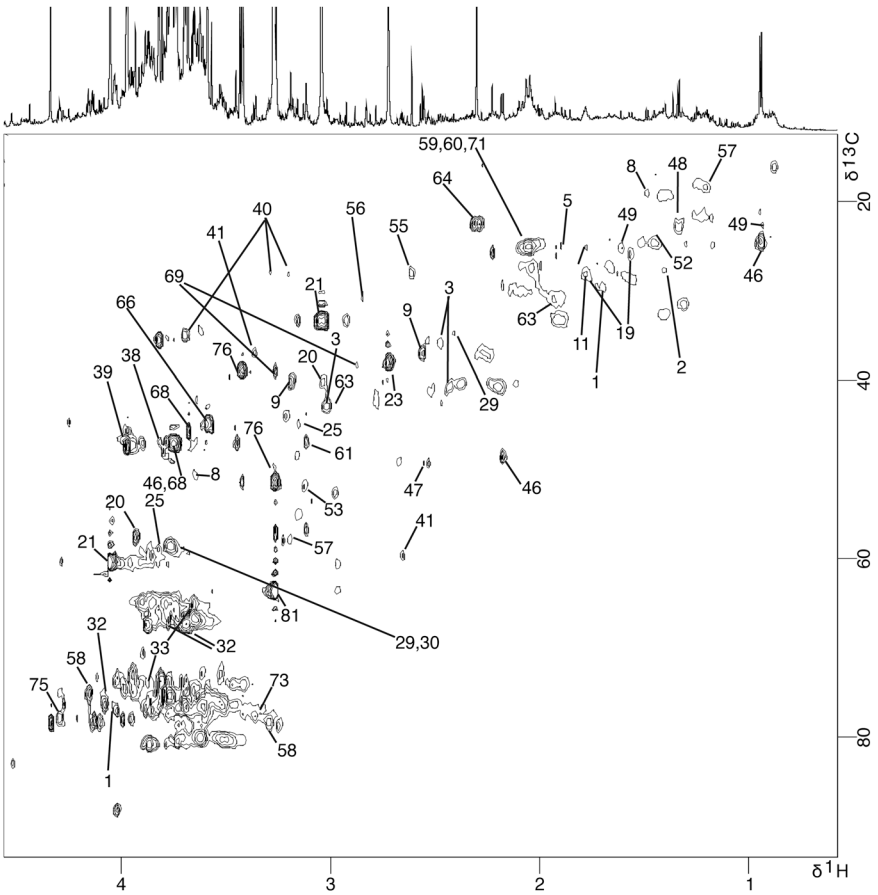

Fig. 3 800 MHz ^{1}H–^{13}C HSQC NMR spectrum of urine. Key as indicated by Table 1.

Tyrosine, as in most mammals has *p*-cresol as a major metabolic end point. *p*-Cresol is a known gut-microbial metabolite linked to clostridial, bacteroidal and bifidobacterial species in particular[15,29,30] and is glucuronidated in the pig, rather than sulfated as it is in man,[15] rodents are known to conjugate *p*-cresol with both sulfate and glucuronide.[31] This result is consistent with prior observations that the pig is 'defective in sulfation' for some aromatic compounds.[29] As observed previously, the pig excretes relatively more *p*-cresol than humans or rodents.[23,32] Phenylacetate, derived from dietary phenylalanine[15] is conjugated with glycine in the pig, consistent with prior reports that all mammals except man and old world monkeys conjugate this microbial metabolite with glycine, with humans producing phenylacetylglutamine.[33]

Materials and methods

Animal husbandry

As part of a wider study on nutritional intervention in weanling white landrace pigs, urine, serum, liver and kidney samples from a healthy mixed gender (4 boars and 3 gilts) conventional group (n = 7) were obtained at post-mortem conducted at the School of Clinical Veterinary Sciences (Bristol University, Langford). Animal housing and experimental procedures were all performed according to local ethical guidelines: all experiments were performed under a UK Home Office Licence and were approved by the local ethical review group. At 3 weeks of age, the piglets were weaned onto a soya-based diet supplemented with appropriate levels of vitamins and minerals, manufactured to order by Parnutt Foods Ltd (Sleaford, Lincolnshire, UK). From 7 weeks old, piglets were fed a fish-based diet and at 9 weeks old, all piglets received a systemic challenge of 2 mg ovalbumin and 2 mg Quil A in 2 ml PBS by intra-peritoneal (I.P.) injection. Quil A acts as an adjuvant, and can transiently stimulate the immune system. This effect is unlikely to have an effect on the metabolic profile at the time of tissue collection however, and this intervention can be considered to be equivalent to a vaccination, common to the young pig and infant. Pigs were euthanased at 11 weeks by injection with Stresnil® (Azaperone) to act as a sedative followed by intra-venous injection of Euthatal® (Pentobarbitone). Blood was drawn from the jugular vein immediately post-mortem, centrifuged, and serum was aliquotted and frozen at −40 °C. Urine was removed immediately by direct extraction from the bladder *via* sterile syringe and snap-frozen. 1 cm^3 sections from the tip of the left lobe of the liver, and from the cortex of the left kidney were excised and snap-frozen in liquid nitrogen within 15 min post-mortem. Tissue samples were stored at −80 °C and urine and serum samples at −40 °C pending NMR analysis.

Sample preparation

Blood serum samples were prepared by adding a 0.9% saline solution containing 10% D_2O (to act as a spectrometer field frequency lock) to 200 μl of blood serum making a total volume of 550 μl. Urine samples were prepared by adding

Table 1 ^{1}H and ^{13}C NMR peak assignments for identified metabolites[a]

No.	Compound	Assignment	δ^{1}_{H}	Multiplicity	δ^{13}_{C}	Confirmation	Compartment
1	2-Hydroxybutyrate	CH_3	0.9	t	11.5	1D, JRES, TOCSY	U,S
		CH_2	1.7	m	29.8		
		CH	4	dd	76.2		
2	2-Hydroxyisobutyrate	$2xCH_3$	1.36	s	29.3	1D, JRES, HSQC	U,S
3	2-Oxoglutarate	γCH_2	2.44	t	33.9	1D, JRES, TOCSY, HSQC	U,S
		βCH_2	3.01	t	39.6		
4	3-Aminoisobutyrate	CH_3	1.18	d	17.8	1D, JRES, TOCSY	U
		CH	2.60	m	42.1		
		CH_2	3.02	dd	45.1		
		CH_2	3.09	dd	45.1		
5	Acetate	CH_3	1.92	s	24.9	1D, JRES, HSQC	U,S,L,K
6	Acetone	CH_3	2.23	s	32.7	1D, JRES	U,S
7	Adenine	H8	8.19	s	152.4	1D, JRES, HSQC, STOCSY	U
		H2	8.21	s	152.7		
8	Alanine	βCH_3	1.46	d	18.8	1D, JRES, TOCSY, HSQC	U,S,L,K
		αCH	3.78	q	53.9		
9	β-Alanine	CH_2COOH	2.56	t	36.5	1D, JRES, TOCSY	U,S,L,K
		$N–CH_2$	3.19	t	39.5		
10	Albumin lysyl	CH_2	2.89	t	40.0*	1D, JRES, HSQC	S
		CH_2	2.96	t	40.0*		
		CH_2	3.01	t	40.0*		
11	Arginine	γCH_2	1.66	m	27.3	1D, JRES, TOCSY, HSQC, STOCSY	U,S,L,K
		βCH_2	1.91	m	30.8		
		δCH_2	3.27	t	43.4		
		αCH	3.77	t	58.6		
12	Ascorbate	CH_2	3.73	m	66.9	1D, JRES, TOCSY, HSQC	L
		CH	4.01	ddd	72.2		
		C5	4.51	d	81.0		
13	Asparagine	$\frac{1}{2}\beta CH_2$	2.86	dd	37.3	1D, JRES, TOCSY	L,K
		$\frac{1}{2}\beta CH_2$	2.96	dd	37.4		
		αCH	4.00	dd	54.1*		
14	Aspartate	$\frac{1}{2}\beta CH_2$	2.68	dd	39.3	1D, JRES, TOCSY, HSQC	L,K
		$\frac{1}{2}\beta CH_2$	2.82	dd	39.4		
		αCH	3.91	dd	55.1*		
15	Betaine	$N–(CH_3)_3$	3.27	s	51.9	1D, JRES, TOCSY, HSQC, STOCSY	S,K
		CH_2	3.93	s	68.6		
16	Cholesterol	C18 (in HDL)	0.66	m	12.6	1D, JRES, HSQC	S
		C18 (in VLDL/LDL)	0.70	m	~		
		C26,C27	0.84	m	23.3*		
		C21	0.91	~	19.4*		
17	Choline	$N–(CH_3)_3$	3.22	s	58.2	1D, JRES, TOCSY, HSQC	U,S,L,K
		βCH_2	3.53	dd	72.8		
		αCH_2	4.06	t	58.4		
18	Citrate	$\frac{1}{2}\gamma CH_2$	2.55	d	40.6	1D, JRES, TOCSY	U,S
		$\frac{1}{2}\gamma CH_2$	2.7	d	40.6		
19	Citrulline	γCH_2	1.57	m	25.9	1D, JRES, HSQC, TOCSY	U,S,K
		βCH_2	1.86	m	28.2		
		δCH_2	3.15	q	42.0		
		αCH	3.76	t	58.5		
20	Creatine	$N–CH_3$	3.03	s	40.4	1D, JRES, TOCSY, HSQC	U,S,L,K
		$N–CH_2$	3.94	s	57.7		
21	Creatinine	$N–CH_3$	3.05	s	30.5	1D, JRES, TOCSY, HSQC	U,S
		$N–CH_2$	4.06	s	56.8		
22	Cysteine	βCH_2	3.03	dd	27.7*	1D, JRES, HSQC	K
		αCH	3.97	t	58.8*		
23	Dimethylamine	CH_3	2.72	s	37.3	1D, HSQC	U,S,K
24	Dimethylglycine	CH_3	2.93	s	47.5	1D, HSQC	U
		CH_2	3.71	s	62.6*		
25	Ethanolamine	CH_2NH_2	3.13	t	44.8	1D, JRES, TOCSY, HSQC	U,L,K
		CH_2OH	3.83	t	60.2		
26	Formate	HCOOH	8.46	s	~	1D	U,S
27	α-Glucose	C4H	3.42	m	72.9	1D, JRES, TOCSY, HSQC, STOCSY	U,S,L,K
		C2H	3.54	m	72.2		
		C3H	3.72	m	75.9		
		$\frac{1}{2}$-C6H_2	3.73	m	63.8		
		$\frac{1}{2}$-C6H_2	3.77	m	64.0		
		C5H	3.87	m	70.1		
		C1H	5.23	d	92.5		
28	β-Glucose	C2H	3.25	m	77.1	1D, JRES, TOCSY, HSQC, STOCSY	U,S,L,K
		C4H	3.49	m	69.8		

Table 1 (*continued*)

No.	Compound	Assignment	δ^1_H	Multiplicity	δ^{13}_C	Confirmation	Compartment
		C5H	3.49	m	79.0		
		C3H	3.50	m	79.0		
		$\frac{1}{2}$-C6H_2	3.88	m	61.1		
		$\frac{1}{2}$-C6H_2	3.91	d	63.9		
		C1H	4.66	d	96.1		
29	Glutamate	βCH_2	2.02	m	29.8	1D, JRES, TOCSY, HSQC, STOCSY	U,S,L,K
		γCH_2	2.34	m	36.3		
		αCH	3.76	dd	57.6		
30	Glutamine	βCH_2	2.15	m	29.2	1D, JRES, TOCSY, HSQC, STOCSY	U,S,L,K
		γCH_2	2.44	m	33.9		
		αCH	3.77	t	57.2		
31	Glutathione	CH_2	2.17	m	29*	1D, STOCSY	L
		CH_2	2.53	m	34*		
		S–CH_2	2.95	dd	28.3*		
		N–CH	3.83	m	46*		
		CH	4.56	q	58.5*		
32	Glycerate	$\frac{1}{2}CH_2$	3.72	dd	66.9	1D, JRES, TOCSY, HSQC	U
		$\frac{1}{2}CH_2$	3.83	dd	66.9		
		CH	4.09	dd	76.1		
33	Glycerol	$\frac{1}{2}CH_2$	3.58	m	65.4	1D, JRES, TOCSY, HSQC	U,S,L,K
		$\frac{1}{2}CH_2$	3.62	m	65.4		
		CH	3.77	t	74.9		
34	Glycerophosphocholine	N–$(CH_3)_3$	3.22	s	56.6*	1D, JRES, TOCSY	S,L,K
		NCH_2	3.68	m	62*		
		OCH_2	4.32	m	64.6*		
35	Glycine	αCH_2	3.55	s	44.1	1D, HSQC	U,S,L,K
36	Glycogen	C2H	3.63	dd	72.6*	1D, JRES, TOCSY, HSQC	L
		C4H	3.66	dd	77.4*		
		C5H	3.83	q	72.3*		
		C6H	3.87	q	61.6*		
		C3H	3.98	d	73.8*		
		C1H	5.41	m(broad)	102.5		
37	Glycolate	CH_2	3.94	s	64.0	1D, JRES, HSQC	K
38	Guanidinoacetate	CH_2	3.8	s	47.4	1D, HSQC	U
39	Hippurate	CH_2	3.98	d	46.7	1D, JRES, TOCSY, HSQC	U
		*m*CH	7.55	t	132.9		
		*p*CH	7.64	t	134.9		
		*o*CH	7.84	d	133.2		
40	Histidines	$\frac{1}{2}CH_2$	3.16	dd	27.6	1D, TOCSY, HSQC	U,S,L,K
		$\frac{1}{2}CH_2$	3.23	dd	27.6		
		CH	3.98	dd	56.1		
		CH	7.09	s	127.0		
		CH	7.90	s	141.1		
41	Hypotaurine	CH_2	2.66	t	58.4	1D, JRES, TOCSY, HSQC	U,L,K
		CH_2	3.34	t	36.2		
42	Hypoxanthine	CH	8.18	s	~	1D, STOCSY	L,K
		CH	8.21	s	~		
43	Indoleacetylglycine (IAG)	CH_2	3.73	s	~	1D, STOCSY, HSQC	U
		CH_2	3.82	s	~		
		C6H	7.19	t	125.5		
		C5H	7.28	t	128.0		
		C2H	7.35	s	133.4		
		C7H	7.55	d	134.9		
		C4H	7.64	d	138.1		
44	Isoleucine	γCH_3	0.94	t	14.2	1D, JRES, HSQC, STOCSY	U,S,L,K
		δCH_3	1.02	d	17.3		
		$\frac{1}{2}$γCH_2	1.26	m	26.9		
		$\frac{1}{2}$γCH_2	1.47	ddd	26.9		
		βCH	2.01	m	38.6		
		αCH	3.65	d	62.5		
45	Isovalerate	2xCH_3	0.94	d	24.6	1D, JRES, TOCSY, HSQC	S
		CH	1.94	m	28.8*		
		CH_2	2.07	d	48.0*		
46	Isovalerylglycine	εCH_3	0.94	d	24.3	1D, JRES, TOCSY, HSQC	U
		δCH_2	2.00	d	29.0		
		γCH_2	2.20	d	48.6		
		αCH_2	3.77	s	47.0		
47	Ketoleucine	2xCH_3	0.94	d	24.6	1D, JRES, TOCSY, HSQC	U,S
		CH	2.10	m	27.2		
		CH_2	2.61	d	51.4		

Table 1 (*continued*)

No.	Compound	Assignment	δ^1_H	Multiplicity	δ^{13}_C	Confirmation	Compartment
48	Lactate	βCH_3	1.33	d	22.9	1D, JRES, TOCSY, HSQC	U,S,L,K
		αCH	4.12	q	68.7		
49	Leucine	δCH_3	0.93	d	21.1	1D, JRES, TOCSY, HSQC	U,S,L,K
		βCH_2	0.94	d	22.7		
		γCH	1.71	m	26.7		
		αCH	3.73	m	56.2		
50	Lipids in LDL	$CH_3(CH_2)_n$	0.84	t	23.3	1D, TOCSY, HSQC	S
		$(CH_2)_n$	1.25	m	30.6		
51	Lipids in VLDL	$CH_3CH_2CH_2C=$	0.87	t	14.7	1D, TOCSY, HSQC	S
		$CH_2CH_2CH_2CO$	1.29	m	25.6		
		CH_2CH_2CO	1.57	m			
52	Lysine	γCH_2	1.46	m	22.7	1D, JRES, TOCSY, HSQC, STOCSY	U,S,L,K
		δCH_2	1.71	m	29.6		
		βCH_2	1.84	m	33.2		
		εCH_2	3.01	t	42.2		
53	Malonate	CH_2	3.13	s	51.7	1D, JRES, HSQC	U
54	Methionine	δCH_3	2.13	s	16.5	1D, JRES, TOCSY, HSQC	S,L,K
		βCH	2.14	m	32.7		
		γCH_2	2.60	t	31.5		
		αCH	3.78	t	56.8		
55	Methylamine	CH_3	2.61	s	27.6	1D, JRES, HSQC	U,S
56	Methylguanidine	CH_3	2.81	s	30.4	1D, JRES, HSQC	U
57	Methylmalonate	CH_3	1.22	d	17.9	1D, JRES, TOCSY, HSQC	U
		CH	3.17	q	54.7		
58	*Myo*-Inositol	C5H	3.29	t	77.1	1D, JRES, TOCSY, HSQC	U,S,K
		C1H & C3H	3.53	dd	73.9		
		C4H & C6H	3.63	t	75.1		
		C2H	4.06	t	74.9		
59	*N*-Acetylglycoproteins	$NHCOCH_3$	2.04	s	23.0	1D, JRES, HSQC	U,S
60	*N*-Acetylcysteine	CH_3	2.06	s	25.0	1D, JRES, HSQC	U,S
61	N6,N6,N6-trimethyllysine	$N–CH_2$	3.11	s	46.9	1D, HSQC	U
62	Nicotinurate	CH_2	3.99	s	46.3	1D, JRES, TOCSY	L,K
		H5	7.60	dd	126.7		
		H4	8.25	d	138.9		
		H6	8.71	d	154.2		
		H2	8.94	s	149.9		
63	Ornithine	$\frac{1}{2}\gamma CH_2$	1.72	m	25.5	1D, JRES, TOCSY, HSQC	U,S,L,K
		$\frac{1}{2}\gamma CH_2$	1.82	m	25.5		
		βCH_2	1.93	m	30.3		
		δCH_2	3.04	t	41.8		
		αCH	3.77	t	57.0		
64	*p*-Cresol glucuronide	CH_3	2.30	s	22.0	1D, JRES, TOCSY, STOCSY	U
		C2H & C6H	7.06	m	122.3		
		C3H & C5H	7.23	m	136.5		
65	*p*-Hydroxybenzoate	C3H & C5H	6.97	m	117.0	1D, JRES, TOCSY, HSQC	U
		C2H & C6H	7.76	m	133.0		
66	*p*-Hydroxyphenylacetate	CH_2	3.45	s	46.2	1D, JRES, TOCSY, HSQC	U
		C2H & C6H	6.87	m	118.0		
		C3H & C5H	7.17	m	133.0		
67	*p*-Hydroxyphenylacetylglycine	CH_2	3.58	s	44.6	1D, JRES, TOCSY, HSQC, STOCSY	U
		$N–CH_2$	3.83	d	45.3		
		C2H & C6H	6.88	m	118.6		
		C3H & C5H	7.21	m	135.3		
68	Phenylacetylglycine	CH_2	3.68	s	46.1	1D, JRES, TOCSY, HSQC, STOCSY	U
		CH_2	3.75	d	47.0		
		C2H & C6H	7.37	m	131.2		
		C3H & C5H	7.43	m	135.1		
69	Phenylalanine	$\frac{1}{2}\beta CH_2$	3.12	dd	39.1	1D, JRES, TOCSY, HSQC	U,L,K
		$\frac{1}{2}\beta CH_2$	3.26	dd	39.1		
		C3H & C5H	7.33	m	132.1		
		C4H	7.35	m	130.4		
		C3H & C6H	7.40	m	131.8		
70	Phosphorylcholine	$N–(CH_3)_3$	3.22	s	56.5	1D, JRES, HSQC	L
		OCH_2	3.68	t	60.6		
		NCH_2	4.18	dd	68.9		
71	Proline	γCH_2	2.03	m	26.4	1D, JRES, TOCSY, HSQC	U,S,L,K
		$\frac{1}{2}\beta CH_2$	2.03	m	31.8		
		$\frac{1}{2}\beta CH_2$	2.35	m	31.8		
		$\frac{1}{2}\delta CH_2$	3.38	m	48.9		
		$\frac{1}{2}\delta CH_2$	3.41	m	48.9		
		αCH	4.14	dd	63.9		

Table 1 (*continued*)

No.	Compound	Assignment	δ^1_H	Multiplicity	δ^{13}_C	Confirmation	Compartment
72	Pyruvate	CH_3	2.35	s	29.2	1D, HSQC	S
73	*Scyllo*-Inositol	CH	3.35	s	77.6	1D, HSQC	U,K
74	Serine	αCH	3.85	dd	59.1	1D, JRES, TOCSY, HSQC	K
		$\frac{1}{2}$βCH$_2$	3.95	dd	63.0		
		$\frac{1}{2}$βCH$_2$	3.95	dd	63.0		
75	Tartrate	2CH	4.34	s	77.7	1D, JRES, HSQC	U
76	Taurine	N–CH_2	3.26	t	50.6	1D, JRES, TOCSY, HSQC	U,S,L,K
		S–CH_2	3.43	t	38.9		
77	Threonine	γCH_3	1.32	d	19.5	1D, JRES, COSY, HSQC	U,S,L,K
		αCH	3.6	d	63.4		
		βCH	4.25	m	68.9		
78	Triglycerides	$CH_3(CH_2)_n$	0.9	m	~	1D	L,K
		$(CH_2)_n$	1.29	m	~		
		CH_2–CH_2–CO	1.58	m	~		
		CH_2–C=C	2.04	m	~		
		CH_2–C=O	2.24	m	~		
		=CH·CH_2·CH=	2.75	m	~		
		CH*=$CHCH_2$	5.32	m	~		
79	Trigonelline	CH_3	4.43	s	51.0	1D, HSQC	U
		C4H	8.07	m	130.3		
		C3H & C5H	8.91	m	147.5		
		C1H	9.11	s	148.3		
80	Trimethylamine	CH_3	2.88	s	48.0	1D, HSQC	U,K
81	Trimethylamine-*N*-oxide	N–$(CH_3)_3$	3.27	s	59.9	1D, HSQC	U,S,K
82	Tryptophan	$\frac{1}{2}$βCH$_2$	3.31	dd	29.1	1D, JRES, TOCSY, HSQC	U,L,K
		$\frac{1}{2}$βCH$_2$	3.49	dd	29.1		
		αCH	4.06	dd	57.9		
		C5H	7.21	t	122.1		
		C6H	7.29	t	124.8		
		C1H	7.33	s	127.9		
		C3H	7.55	d	114.7		
		C4H	7.74	d	121.1		
83	Tyrosine	C3H & C5H	6.91	d	118.9	1D, JRES, TOCSY, HSQC	S,L,K
		C2H & C6H	7.19	d	133.5		
84	Uracil	C5H	5.80	d	103.7	1D, JRES, TOCSY, HSQC	L,K
		C6H	7.54	d	146.3		
85	Uridine	$\frac{1}{2}$-CH_2	3.81	dd		1D, JRES, TOCSY	U
		$\frac{1}{2}$-CH_2	3.92	dd	~		
		C4′H	4.12	dt	~		
		C3′H	4.24	dd	~		
		C2′H	4.36	dd	~		
		C1′H	5.88	d	~		
		C5H	5.92	m	~		
		C6H	7.88	d	~		
86	Valine	γCH_3	0.98	d	19.9	1D, JRES, TOCSY, HSQC	U,S,L,K
		γCH_3	1.04	d	21.2		
		βCH	2.27	m	32.2		
		αCH	3.62	d	63.4		

[a] Key: s = singlet, d = doublet, t = triplet, q = quartet, m = multiplet, dd = doublet of doublets, ddd = doublet of doublet of doublets, U = urine, S = serum, K = kidney, L = liver. * Indicates values obtained from the HMDB[47,48]; all other shifts were verified experimentally. The molecule numbering system follows IUPAC rules.

220 μl of a solution of 1 mM sodium 3-trimethylsilyl-1-[2,2,3,3-$^2H_4$]propionate (TSP) and 3 mM sodium azide (NaN_3) in a 80/20 (v/v) H_2O/D_2O 0.1 M phosphate buffer solution (pH 7.4) to 440 μl of urine. The resultant mixture was vortexed, left to stand for ~10 min and then centrifuged at 12 000*g* for 20 min and 600 μl of the resultant supernatant transferred into NMR tubes with an outer diameter of 5 mm.[34] Magic-angle-spinning (MAS) ^{1}H NMR spectroscopy was used to analyse intact tissue samples, which were bathed in a 0.9% saline D_2O solution and a portion (~15 mg) was inserted into a zirconium oxide 4 mm outer diameter rotor, using an insert to make a spherical sample volume of 25 μl.

NMR spectroscopic analysis

Standard 1D spectra were acquired for all samples on an Avance 600 MHz NMR Spectrometer (Bruker Biospin, Coventry, UK). Further metabolite identification was conducted on a sample from a representative male animal chosen based on the quality of the 1D spectra on an Avance 800 MHz NMR Spectrometer (Bruker Biospin, Coventry, UK). ^{1}H, ^{1}H–^{1}H and ^{1}H–^{13}C NMR spectra of serum and urine were recorded with a Bruker 5 mm CP TXI cryoprobe at 300 K. HR-MAS NMR spectroscopy of liver and kidney samples used a 4 mm g-HR MAS HPCD probe for tissue analysis, and a spin rate of

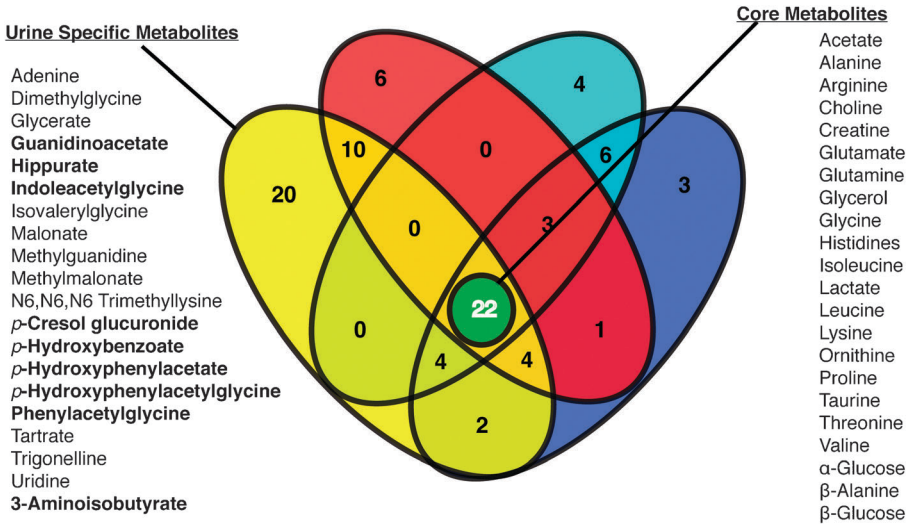

Fig. 4 Venn diagram illustrating the degree of inter-compartmental overlap of metabolic profiles between urine, serum, liver and kidney of the pig. The central section in green represents core metabolites shared between all four compartments; urine-specific metabolites and core metabolites are listed and those in bold represent known or putative gut-microbial co-metabolites (identified from literature research). Compartments are colour coded with urine in yellow, serum in red, liver in cyan and kidney in blue.

5000 Hz was applied. The tissue samples were kept at 283 K during the NMR experiment to minimise time-dependant degradation,[21] but samples were bathed in D_2O prior to the NMR studies and some partial deuteration effects were observed (*vide infra*).

Standard 1D NMR spectra were initially acquired at 600 MHz for all matrices; 256 scans (16 dummy scans) were collected into 64k data points over a 20 ppm spectral width using the first increment of a standard NOE experiment (Bruker pulse program: noesypr1d) with water presaturation during the relaxation delay of 2 s and during the mixing time of 100 ms. A Carr–Purcell–Meiboom–Gill (CPMG) spin-echo spectrum (RD-90°-(D-180°-D)$_n$-acquisition) was recorded for the serum and tissue samples to highlight the contributions of the small molecules with longer T2 relaxation times.[35] Typically, 256 scans (16 dummy scans) were collected into 64k data points over a spectral width of 20 ppm with an acquisition time of 2.044 s and a relaxation delay of 2 s. This sequence incorporated an echo time (D) of 200 μs, which resulted in a total spin echo time of 64 ms for all matrices.

All 2D experiments for assignment were conducted at 800 MHz; two-dimensional *J*-resolved spectroscopy (JRES) was used to elucidate the *J*-coupled multiplicity of peaks for each compound in each matrix; typically 128 scans were collected into 32 increments at a resolution of 64k with an acquisition time of 3.407 s. The spectral width in F1 was 50 Hz and water presaturation was employed during a relaxation delay of 2 s. Spectra were processed using a SINE window function along the F1 and F2 axes with SSB = 0 and a resolution of 64k (in F2) and 128 (F1). The peaks were subsequently tilted by 45° and symmetrised.

Two-dimensional ^{1}H–^{1}H total correlation spectroscopy (TOCSY) spectra were performed using a DIPSI2 sequence for Hartmann–Hahn transfer and excitation sculpting for water suppression.[36–38] Typically 64 transients (32 dummy scans) were collected into 512 increments at a spectral resolution of 8k. Spectra were processed into a resolution of 16k (F2) and 1k (F1) using a shifted QSINE function.

Two-dimensional echo/anti-echo ^{1}H–^{13}C heteronuclear single quantum correlation (HSQC) spectra were collected using a sensitivity improved pulse sequence with adiabatic pulses[39–41] for all matrices. Typically, 320 scans were collected into 128 increments at a spectral resolution of 4k in F2 across a spectral width of 12 ppm and 170 ppm for the ^{1}H and ^{13}C axes respectively, with an acquisition time of 0.852 s and a relaxation delay of 1.2 s; ^{13}C decoupling was achieved using the GARP method,[42] and delays were set for a 145 Hz one-bond ^{1}H–^{13}C coupling constant. Spectra were zero-filled in F2 by a factor of two to 8k, and zero-filling and linear prediction was applied in F1 to result in a resolution of 1k.

Data processing and analysis

An exponential window function with a line broadening of 0.3 Hz was applied prior to Fourier transformation to all 1D NMR spectra, and the resultant spectra were phased, baseline corrected and calibrated to TSP at δ0.0 (urine) or the H1 proton of α-glucose (blood serum & tissues) at δ5.23 manually using Topspin (2.0a, Bruker BioSpin 2006). The spectra (~22k data points) were subsequently imported into MatLab (R2009b, The MathsWorks inc.) where the region containing the water resonance ~(δ4.6–5.2) and for urine, urea ~(δ5.2–5.9) were removed and the spectra were aligned using an algorithm as described previously[43] and normalised using the probabilistic quotient method.[44] Statistical Total Correlation Spectroscopy (STOCSY) and principal components analysis (PCA) were conducted in MatLab (R2009b, The MathsWorks inc.) using an in-house algorithm.[45] STOCSY is a statistical technique employed to view the degree of co-variation between a peak of interest and the rest of the spectrum and can provide information regarding both structural and pathway correlations.[45] This technique was used where assignment of peaks was difficult

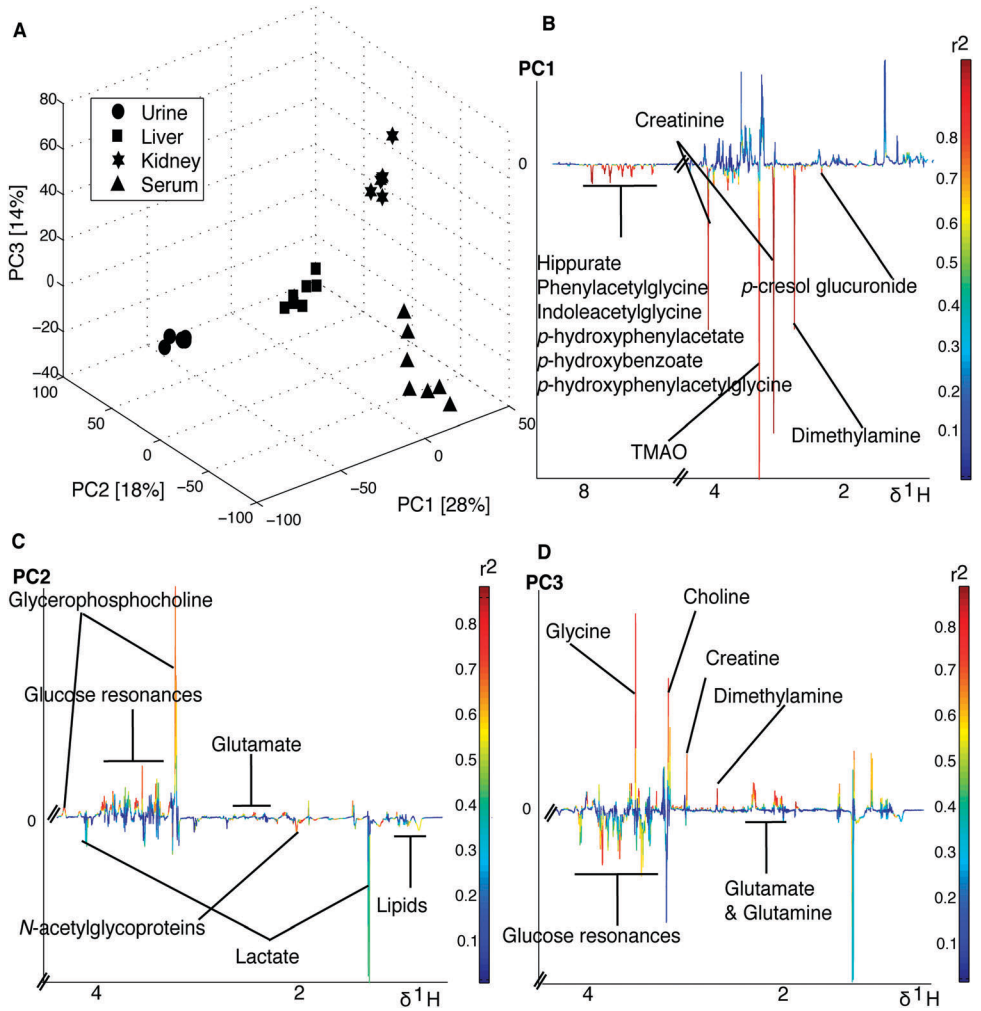

Fig. 5 (A) 3-Dimensional PCA scores plot derived from 600 MHz ^{1}H NMR spectra of urine, serum, liver and kidney from 7 animals, illustrating the inter-compartment spectral variation and the close similarity between spectra of the same biological matrix from different animals. The variance in the first PC is mainly dominated by differences in the urinary biochemical composition with respect to all other tissues. (B) PCA loadings representing the metabolic variation in PC1 relating to the difference between urine and the other biomatrices. Loadings are displayed by a back-scaled covariance matrix of the PCA loadings projected onto a pseudo-spectrum and colour coded by the weight of the loading. Those NMR resonances pointing downwards are relatively increased in urine comparative to the other biological compartments. (C) Displays the spectral variables responsible for the metabolic variation along PC2 mainly driven by the differences between liver and serum, resonances pointing up are relatively increased in liver comparative to serum and (D) PC3 predominantly describing differences between kidney and serum/liver with resonances pointing upwards being relatively higher in kidney comparative to serum and liver.

to provide further information about the resonance in question and for confirmation of assignments.

Literature[16,46] or databases such as the Human Metabolome Data Base (HMDB): http://hmdb.ca/,[47,48] or the Biological Magnetic Resonance Data Bank (BMRB): http://www.bmrb.wisc.edu, along with SBase/Amix (Bruker BioSpin 2006) were used to provide candidate molecules for unassigned NMR resonances.

In order to show the commonality of metabolites between the various biological matrices, a Venn diagram was created using Venny software.[49]

Conclusions

Urine was found to contain the most distinct and comprehensive set of metabolites, with at least 62 NMR visible (and assignable) metabolites compared to 47 in serum, 45 kidney and 39 in the liver. The urinary metabotype of the pig provides additional information relating to diet and to end-products of gut-microbial co-metabolism and therefore provides the best window on the mammalian ecosystem, which includes resident organisms such as bacteria and fungi that interact with the host and increase the metabolic capacity and diversity of the host. This information provides an idea of species differences relating to phase II metabolism in the pig. These inter-species differences are important observations to note during data interpretation and when considering the translatability of metabonomics in animal experiments to the metabolic response in humans, as the peaks observable in the NMR spectra differ depending on the route of phase II conjugation.

The results highlight the importance of collecting urine during intervention studies if information regarding the

activity of the gut microbiome is desired. In addition, this study validates the use of biofluids such as serum and urine to retrieve information regarding host energy metabolism and extra-genomic metabolism, as the major metabolic endpoints of both these processes dominate the NMR spectrum. The relative similarities of pigs to humans in terms of conserved metabolic composition renders them a suitable model for continued metabonomic investigation, provided species differences in phase II metabolism are accounted for. This endorses the use of metabonomics to non-invasively monitor dietary intervention studies in this species, thereby potentially enhancing information recovery from animal experiments concerned with investigating the highly complex synergistic relationship between mammals and microbes.

Acknowledgements

The authors would like to thank Dr Jake TM Pearce and Dr Rachel Cavill for helpful discussions. CAM, SPC and MED thank Nestlé for financial support through the Imperial College London/Nestlé strategic alliance (RDLS015375).

References

1 E. R. Miller and D. E. Ullrey, *Annu. Rev. Nutr.*, 1987, **7**, 361–382.
2 M. Bailey, K. Haverson, C. Inman, C. Harris, P. Jones, G. Corfield, B. Miller and C. Stokes, *Proc. Nutr. Soc.*, 2005, **64**, 451–457.
3 L. K. Bustad and R. O. McClellan, *Science*, 1966, **152**, 1526–1530.
4 S. N. Meyers, M. B. Rogatcheva, D. M. Larkin, M. Yerle, D. Milan, R. J. Hawken, L. B. Schook and J. E. Beever, *Genomics*, 2005, **86**, 739–752.
5 M. B. Rogatcheva, K. Chen, D. M. Larkin, S. N. Meyers, B. M. Marron, W. He, L. B. Schook and J. E. Beever, *Animal Biotechnology*, 2008, **19**, 28–42.
6 R. Forster, P. Ancian, M. Fredholm, H. Simianer and B. Whitelaw, *J. Pharmacol. Toxicol. Methods*, 2010, **62**, 227–235.
7 M. Uchida, Y. Shimatsu, K. Onoe, N. Matsuyama, R. Niki, J. E. Ikeda and H. Imai, *Transgenic Research*, 2001, **10**, 577–582.
8 J. K. Nicholson, J. C. Lindon and E. Holmes, *Xenobiotica*, 1999, **29**, 1181–1189.
9 A. N. Phipps, J. Stewart, B. Wright and I. D. Wilson, *Xenobiotica*, 1998, **28**, 527–537.
10 M. T. Yokoyama and J. R. Carlson, *The American Journal of Clinical Nutrition*, 1979, **32**, 173–178.
11 S. H. Zeisel, K. A. DaCosta and J. G. Fox, *The Biochemical Journal*, 1985, **232**, 403–408.
12 S. H. Zeisel, K. A. DaCosta, M. Youssef and S. Hensey, *The Journal of Nutrition*, 1989, **119**, 800–804.
13 S. H. Zeisel, J. S. Wishnok and J. K. Blusztajn, *The Journal of Pharmacology and Experimental Therapeutics*, 1983, **225**, 320–324.
14 S. C. Mitchell, A. Q. Zhang and R. L. Smith, *Food and Chemical Toxicology: An International Journal Published for the British Industrial Biological Research Association*, 2008, **46**, 1734–1738.
15 E. A. Smith and G. T. Macfarlane, *Journal of Applied Bacteriology*, 1996, **81**, 288–302.
16 J. K. Nicholson, P. J. Foxall, M. Spraul, R. D. Farrant and J. C. Lindon, *Anal. Chem.*, 1995, **67**, 793–811.
17 B. Martinez-Granados, D. Monlein, M. C. Martinez-Bisbal, J. M. Rodrigo, J. del Olmo, P. Lluch, A. Ferrindez, L. Marti-Bonmati and B. Celda, *NMR Biomed.*, 2006, **19**, 90–100.
18 M. E. Bollard, S. Garrod, E. Holmes, J. C. Lindon, E. Humpfer, M. Spraul and J. K. Nicholson, *Magn. Reson. Med.*, 2000, **44**, 201–207.
19 D. A. Dalton, S. A. Russell, F. J. Hanus, G. A. Pascoe and H. J. Evans, *Proc. Natl. Acad. Sci. U. S. A.*, 1986, **83**, 3811–3815.
20 M. L. Anthony, C. R. Beddell, J. C. Lindon and J. K. Nicholson, *J. Pharm. Biomed. Anal.*, 1993, **11**, 897–902.
21 N. J. Waters, S. Garrod, R. D. Farrant, J. N. Haselden, S. C. Connor, J. Connelly, J. C. Lindon, E. Holmes and J. K. Nicholson, *Anal. Biochem.*, 2000, **282**, 16–23.
22 M. E. Bollard, E. G. Stanley, J. C. Lindon, J. K. Nicholson and E. Holmes, *NMR Biomed.*, 2005, **18**, 143–162.
23 M. T. Yokoyama, C. Tabori, E. R. Miller and M. G. Hogberg, *The American Journal of Clinical Nutrition*, 1982, **35**, 1417–1424.
24 M. al-Waiz, M. Mikov, S. C. Mitchell and R. L. Smith, *Metabolism: Clinical and Experimental*, 1992, **41**, 135–136.
25 S. Rezzi, Z. Ramadan, L. B. Fay and S. Kochhar, *J. Proteome Res.*, 2007, **6**, 513–525.
26 W. R. Wikoff, A. T. Anfora, J. Liu, P. G. Schultz, S. A. Lesley, E. C. Peters and G. Siuzdak, *Proc. Natl. Acad. Sci. U. S. A.*, 2009, **106**, 3698–3703.
27 I. Bertini, A. Calabra, V. De Carli, C. Luchinat, S. Nepi, B. Porfirio, D. Renzi, E. Saccenti and L. Tenori, *J. Proteome Res.*, 2009, **8**, 170–177.
28 D. H. Bueschkens and M. E. Stiles, *Applied and Environmental Microbiology*, 1984, **48**, 601–605.
29 B. L. Goodwin, C. R. Ruthven and M. Sandler, *Biochem. Pharmacol.*, 1994, **47**, 2294–2297.
30 M. Li, B. Wang, M. Zhang, M. Rantalainen and S. Wang, *Proc. Natl. Acad. Sci. U. S. A.*, 2008, **105**, 2117–2112.
31 E. Bohus, M. Coen, H. C. Keun, T. M. D. Ebbels, O. Beckonert, J. C. Lindon, E. Holmes, B. Noszál and J. K. Nicholson, *J. Proteome Res.*, 2008, **7**, 4435–4445.
32 S. F. Spoelstra, *Applied and Environmental Microbiology*, 1978, **36**, 631–638.
33 R. T. Williams, *Environ. Health Perspect.*, 1978, **22**, 133–138.
34 O. Beckonert, H. C. Keun, T. M. D. Ebbels, J. Bundy, E. Holmes, J. C. Lindon and J. K. Nicholson, *Nat. Protoc.*, 2007, **2**, 2692–2703.
35 S. Meiboom and D. Gill, *Rev. Sci. Instrum.*, 1958, **29**, 688–691.
36 S. R. Hartmann and E. L. Hahn, *Phys. Rev.*, 1962, **128**, 2042.
37 A. J. Shaka, D. N. Shykind, G. C. Chingas and A. Pines, *J. Magn. Reson.*, 1988, **80**, 96–111.
38 T. L. Hwang and A. J. Shaka, *J. Magn. Reson.*, 1998, **135**, 280–287.
39 J. Cavanagh, A. G. Palmer, P. E. Wright and M. Rance, *J. Magn. Reson.*, 1991, **91**, 429–436.
40 L. E. Kay, P. Keifer and T. Saarinen, *J. Am. Chem. Soc.*, 1992, **114**, 10663–10665.
41 J. Schleucher, M. Schwendinger, M. Sattler, P. Schmidt, O. Schedletzky, S. J. Glaser, O. W. Sorensen and C. Griesinger, *J. Biomol. NMR*, 1994, **4**, 301–306.
42 A. J. Shaka, P. B. Barker and R. Freeman, *J. Magn. Reson.*, 1985, **64**, 547–552.
43 K. A. Veselkov, J. C. Lindon, T. M. Ebbels, D. Crockford, V. V. Volynkin, E. Holmes, D. B. Davies and J. K. Nicholson, *Anal. Chem.*, 2009, **81**, 56–66.
44 F. Dieterle, A. Ross, G. Schlotterbeck and H. Senn, *Anal. Chem.*, 2006, **78**, 4281–4290.
45 O. Cloarec, M. E. Dumas, A. Craig, R. H. Barton, J. Trygg, J. Hudson, C. Blancher, D. Gauguier, J. C. Lindon, E. Holmes and J. Nicholson, *Anal. Chem.*, 2005, **77**, 1282–1289.
46 W. M. T. Fan, *Progress in Nuclear Magnetic Resonance Spectroscopy*, 1996, **28**, 161–219.
47 D. S. Wishart, C. Knox, A. C. Guo, R. Eisner, N. Young, B. Gautam, D. D. Hau, N. Psychogios, E. Dong, S. Bouatra, R. Mandal, I. Sinelnikov, J. Xia, L. Jia, J. A. Cruz, E. Lim, C. A. Sobsey, S. Shrivastava, P. Huang, P. Liu, L. Fang, J. Peng, R. Fradette, D. Cheng, D. Tzur, M. Clements, A. Lewis, A. De Souza, A. Zuniga, M. Dawe, Y. Xiong, D. Clive, R. Greiner, A. Nazyrova, R. Shaykhutdinov, L. Li, H. J. Vogel and I. Forsythe, *Nucleic Acids Res.*, 2009, **37**, D603–D610.
48 D. S. Wishart, D. Tzur, C. Knox, R. Eisner, A. C. Guo, N. Young, D. Cheng, K. Jewell, D. Arndt, S. Sawhney, C. Fung, L. Nikolai, M. Lewis, M. Coutouly, I. Forsythe, P. Tang, S. Shrivastava, K. Jeroncic, P. Stothard, G. Amegbey, D. Block, D. D. Hau, J. Wagner, J. Miniaci, M. Clements, M. Gebremedhin, N. Guo, Y. Zhang, G. E. Duggan, G. D. MacInnis, A. M. Weljie, R. Dowlatabadi, F. Bamforth, D. Clive, R. Greiner, L. Li, T. Marrie, B. D. Sykes, H. J. Vogel and L. Querengesser, *Nucleic Acids Research*, 2007, **35**, D521–D526.
49 J. C. Oliveros, in http://bioinfogp.cnb.csic.es/tools/venny/index.html, 2007.

